Electron Spin Dynamics of Photoexcited Corannulene–Lithium Complexes in Tetrahydrofuran. Fourier Transform Electron Paramagnetic Resonance

Gil Zilber,[‡,§] Vladimir Rozenshtein,[‡] Pei-Chao Cheng,[†] Lawrence T. Scott,[†] Mordecai Rabinovitz,[*,§] and Haim Levanon[*,‡]

Contribution from the Department of Physical Chemistry, the Farkas Center for Light-Induced Processes, and the Department of Organic Chemistry, The Hebrew University of Jerusalem, Jerusalem 91904, Israel, and Merkert Chemistry Center, Department of Chemistry, Boston College, Chestnut Hill, Massachusetts 02167-3860

Received June 16, 1995[®]

Abstract: Tetrahydrofuran (THF) solutions of corannulene (Cor) reduced by lithium metal exhibit electron paramagnetic resonance (EPR) features that depend on the reduction stage of Cor, the temperature, and the nuclear spin (isotope effect). Photoexcitation of these solutions results in EPR emissive spectra, attributed to the trianion, $Cor^{3\bullet-}$, and to the photoelectron, e^-_{photo}. These electron spin polarized (ESP) effects are discussed within the framework of intramolecular electron transfer reactions of ion complexes of highly charged constituents, in conjunction with ESP mechanisms that take into account radical–triplet interactions.

I. Introduction

Photoinduced electron transfer (ET) reactions in non-aqueous solutions, between doubly-charged pyrene and alkali-metal cations (M^+), have been shown to manifest different electron spin polarization (ESP) mechanisms,[1,2] consisting of the correlated radical pair mechanism (CRPM), radical pair mechanism ($S–T_{0,-1}$ RPM), and radical–triplet pair mechanism (RTPM). In these studies, the ESP effects were found to be of temporal behavior and to depend on the alkali-metal and ion-solvation state, with unique features due to the Coulombic interaction of the charged species that strongly affects the in-cage lifetime of the radical pair and the diffusion rate.[1,2] A different example of an electrostatically-bound complex is that of corannulene (Cor) interacting with alkali metals.

Corannulene (Cor) with its bowl shaped structure (Figure 1)[3] is the minimal subunit of C_{60} and the higher fullerenes that maintains a curve molecular surface.[4] Cor was first synthesized in 1966[5] and was investigated together with its radical anion[6] and photoexcited triplet state.[7] New synthetic methods[8,9] and the redox reactions of Cor with Li to produce the Cor tetraanion dimer[10] have stimulated us to further study the Cor/Li system
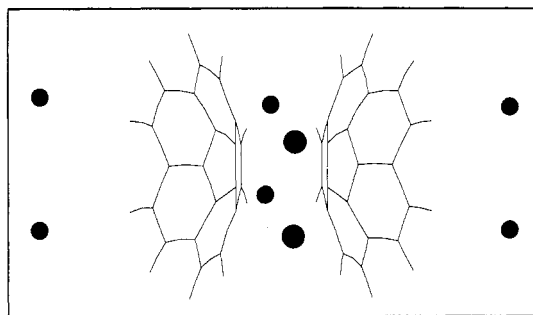
Figure 1. Ion-bonded dimer structure of Cor/Li as suggested by NMR data (see text). Circles represent lithium cations.

in non-aqueous media, focussing on the paramagnetic intermediates and their participation in photoinduced ET reactions in this system.

We report here some conspicuous CIDEP (chemically induced dynamic electron polarization) effects found in photoexcited Cor/Li/THF solutions. The process under investigation is a special case of geminate reactions involving systems that are ionically bound, where the collisions to form cage complexes are not required. In other words, we consider here the effect of the magnetic field on spin pairs, subjected to diffusion and reencounters within the cage. In these systems, the net emissive spectra are attributed to the polarized photoelectron, e^-_{photo}, and the radical trianion, $Cor^{3\bullet-}$, that are associated with the photoinduced ET reactions within these complexes. To explain these observations, we discuss several possible CIDEP mechanisms, such as the RPM ($S–T_{-1}$), triplet mechanism (TM), and RTPM.

II. Experimental Section

Corannulene was synthesized by FVP (flash vacuum pyrolysis) and purified chromatographically.[8] THF (tetrahydrofuran, Aldrich Chemicals) was dried over Na/K alloy. Samples of Cor/M/THF solutions were prepared under vacuum after a long contact with the alkali-metal mirror or a wire for the case of Li. The experimental setup for the pulsed Fourier transform EPR (FT-EPR) measurements (X-band) following pulsed laser excitation was described in detail previously.[2]

† Merkert Chemistry Center, Department of Chemistry, Boston College.
‡ Department of Physical Chemistry and the Farkas Center for Light-Induced Processes, The Hebrew University of Jerusalem.
§ Department of Organic Chemistry, The Hebrew University of Jerusalem.
® Abstract published in *Advance ACS Abstracts*, October 1, 1995.
(1) Zilber, G.; Rozenshtein, V.; Levanon, H.; Rabinovitz, M. *Chem. Phys. Lett.* **1992**, *196*, 255.
(2) Rozenshtein, V.; Zilber, G.; Robinovitz, M.; Levanon, H. *J. Am. Chem. Soc.* **1993**, *115*, 5193.
(3) Hanson, J. C.; Nordman, C. E. *Acta Crystallogr.* **1976**, *B32*, 1147.
(4) Kroto, H. W.; Allaf, A. W.; Balm, S. P. *Chem. Rev.* **1991**, *91*, 1213.
(5) Barth, W. E.; Lawton, R. G. *J. Am. Chem. Soc.* **1966**, *88*, 380.
(6) Janata, J.; Gendell, J.; Ling, C.-Y.; Barth, W.; Backes, L.; Mark, H. B., Jr.; Lawton, R. G. *J. Am. Chem. Soc.* **1967**, *89*, 3056.
(7) Bramwell, F. B.; Gendell, J. *J. Chem. Phys.* **1970**, *52*, 5656.
(8) Scott, L. T.; Hashemi, M. M.; Meyer, D. T.; Warren, H. B. *J. Am. Chem. Soc.* **1991**, *113*, 7082.
(9) Borchardt, A.; Fuchicello, A.; Kilway, K. V.; Baldridge, K. K.; Siegel, J. S. *J. Am. Chem. Soc.* **1992**, *114*, 1921.
(10) Ayalon, A.; Sygula, A.; Cheng, P.-C.; Rabinovitz, M.; Rabideau, P. W.; Scott, L. T. *Science* **1994**, *256*, 1065.
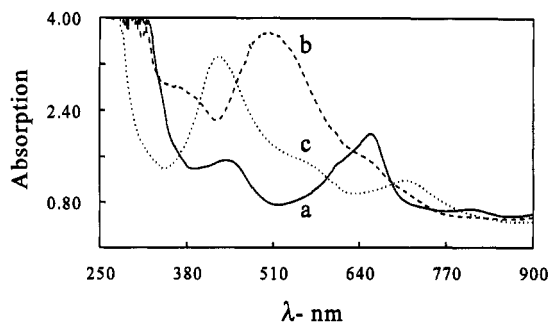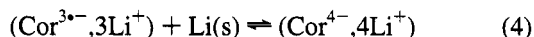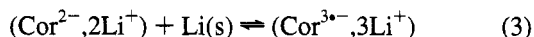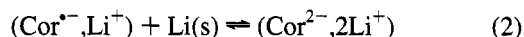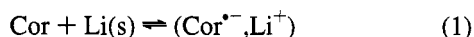
Figure 2. UV—visible absorption spectra of the Cor/Li/THF solution for different reduction stages that exhibit different colored solutions green (a); purple (b); and brown (c).

Experiments were carried out using a pulsed (24 ns microwave pulses) EPR spectrometer (Bruker ESP 380) interfaced to a Nd-YAG laser (Continuum, Model 661-2D) with light pulses of 20 Hz repetition rate, ~75 mJ/pulse, 12 ns pulse width, at $\lambda = 532$ nm. Free induction decay (FID) signals were detected at selected delay times (τ_d) after the laser pulse. The spectra of equilibrated Cor radicals, taken in the absence of light irradiation, were used as references for phase correction of the spin-polarized spectra. Characterization of the spin-equilibrated systems was carried out by conventional CW-EPR detection (100 kHz field modulation), UV—visible absorption spectroscopy, and NMR.
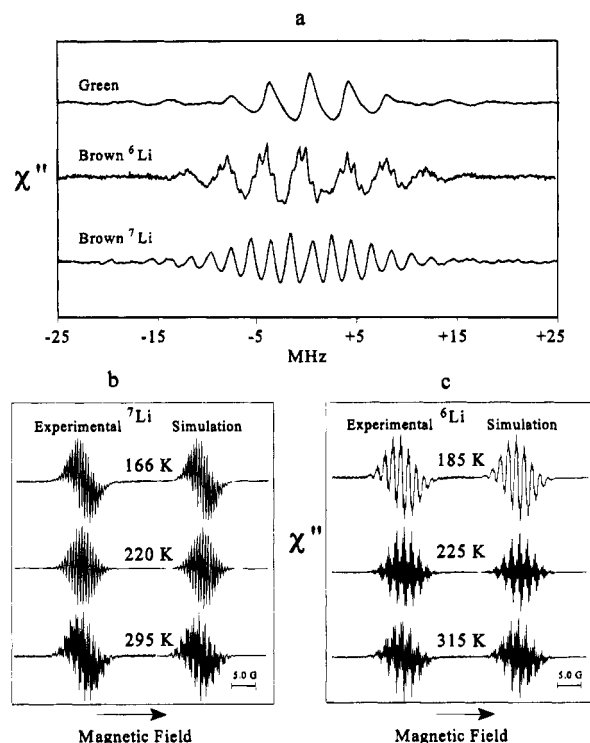
III. Results and Discussion

A. Characterization of Cor/Li/THF Solutions in Equilibrium.
It has already been shown that Cor in Cor/Li/THF solutions is reduced in a multistep process, leading to the formation of a stable tetralithium salt $(Cor^{4-},4Li^{+})$.[11] In the case of the other reducing metals (sodium, potassium, or rubidium) only two reduction steps were observed. The color changes with time, associated with the different reduction states, are green (a few hours), to purple (days), to the stable brown color solution.[11] While the green and the purple solutions are common to Li, Na, K, and Rb, the brown color is typical of the Cor/Li/THF solution only. Therefore, we confine our study to the Li metal.

The following reactions depict the successive reduction stages of Cor with Li:

$$Cor + Li(s) \rightleftharpoons (Cor^{\bullet-},Li^{+}) \qquad (1)$$

$$(Cor^{\bullet-},Li^{+}) + Li(s) \rightleftharpoons (Cor^{2-},2Li^{+}) \qquad (2)$$

$$(Cor^{2-},2Li^{+}) + Li(s) \rightleftharpoons (Cor^{3\bullet-},3Li^{+}) \qquad (3)$$

$$(Cor^{3\bullet-},3Li^{+}) + Li(s) \rightleftharpoons (Cor^{4-},4Li^{+}) \qquad (4)$$

where s stands for the solid state.

The UV—visible absorption spectra of Cor/Li/THF solutions as a function of the reduction stage are presented in Figure 2. The green solution is typified by the absorption maxima at 430, 620, 650, and 800 nm, the purple solution is characterized by the absorptions at 375 and 512 nm, and the brown solution is characterized by 425, 525, 575, and 710 nm. As confirmed by the EPR spectra, the green solution contains mainly the $Cor^{\bullet-}$ species (eq 1), and the 650 nm absorption peak is due to this anion radical.[6] The purple solution is mainly due to $(Cor^{2-},2M^{+})$ with some remnant of the monoanion.[12] Moreover, the absence of the 650-nm maximum in the absorption spectrum of the brown solution indicates that $Cor^{\bullet-}$ is absent, and the EPR

(11) Ayalon, A.; Rabinovitz, M.; Cheng, P. C.; Scott, L. T. *Angew. Chem., Int. Ed. Engl.* **1992**, *31*, 1636.

(12) Baumgarten, M.; Gherghel, L.; Wagner, M.; Weitz, A.; Rabinovitz, M.; Cheng, P. C.; Scott, L. T. *J. Am. Chem. Soc.* Submitted for publication.

Figure 3. (a) FT-EPR spectra (at 167 K) of $Cor^{\bullet-}$ (green solution) and Cor^{3-} (brown solution). The latter solutions were prepared with ^6Li or ^7Li (see text). (b and c) Experimental and simulated CW-EPR spectra of Cor^{3-} at different temperatures and Li isotopes.

spectra, which were detected in the brown solutions (see next section), may be assigned to the trianion radical, $Cor^{3\bullet-}$, that coexists with Cor^{4-} (eqs 3 and 4).[12] As confirmed by the NMR studies, the brown Cor/Li/THF solution includes the stable dimeric form of the tetraanion, Cor^{4-}, in which the four electrons are delocalized over the entire carbon skeleton of Cor^{4-}.[10,11]

B. EPR Spectra of Cor/Li/THF Solutions.
Figure 3a exhibits the EPR spectra of Cor/Li/THF solutions under equilibrium at two reduction stages, namely, the green[13] and the brown solutions. The spectra were taken before or a long time after the light irradiation. In both cases, the spectra were found to be identical, although the spectra of the brown solutions following the light excitation were found to be more intense. This observation indicates that by photoexcitation, the formation of radicals is enhanced, which suggests the formation of $Cor^{3\bullet-}$ radicals from Cor^{4-} (see below).

Photoexcitation of the purple solutions results in the appearance of the EPR spectrum of $Cor^{\bullet-}$, which can be attributed to the following process: $(Cor^{2-},2Li^{+}) \rightarrow (Cor^{\bullet-},Li^{+}) + (e^{-}_{photo},Li^{+})$. Thus, in the purple solutions, Cor^{2-} is the main species under equilibrium.[12]

Brown Solution. In the temperature range of 167–350 K, the EPR spectra strongly depend on the nuclear spin of Li, and the temperature, whereas the g-factor remains unchanged, $g_{brown} = 2.0025 \pm 0.0002$. Figure 3 (spectra b and c) shows the experimental and simulated EPR spectra of $Cor/^6Li/THF$ and $Cor/^7Li/THF$ taken at different temperatures. In simulating the spectra several considerations were taken into account: (1) $Cor^{\bullet-}$ does not contribute to the spectrum, since a diamagnetic stage occurs between the formation of $Cor^{\bullet-}$ and $Cor^{3\bullet-}$. Therefore, the spectra are attributed to the trianion radical, $Cor^{3\bullet-}$ $(S = \frac{1}{2})$. (2) Two sets of equivalent nuclei, i.e., 10

(13) The spectra of green solutions are characterized by a g-factor (g_{green} = 2.0027 ± 0.0002) and hyperfine splitting constant (a_{green} = 1.56 ± 0.02 G), due to a set of ten equivalent protons. The results are in full agreement with the previous data for $Cor^{\bullet-}$ species (cf. ref 6).
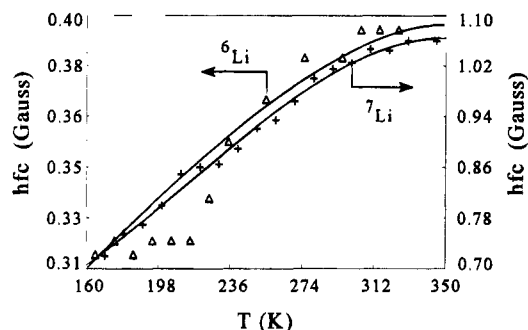
Figure 4. Temperature dependence of ^6Li and ^7Li hfc's of $Cor^{3\bullet-}$ The smooth lines were determined by best-fit fitting.

protons of $Cor^{3\bullet-}$ and 2 lithium nuclei, determine the hyperfine structure of the spectra (Figure 3b,c).

Figure 4 represents the temperature dependence of the alkali-metal hyperfine coupling (hfc) constants, which were obtained via the simulations. The strong temperature effect can be explained in terms of two different ion-pair states within the dimeric complex, i.e., the existence of contact and loose ion pairs.[14] These species are distinguished by the degree of solvation and undergo equilibrium that determines the temperature dependence of the alkali-metal hfc:

$$(Cor^{3\bullet-},Li^+)_l \rightleftharpoons (Cor^{3\bullet-},Li^+)_c \qquad (5)$$
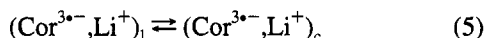
where the subindices l and c stand for loose and contact ion pairs, respectively. Unlike the lifetime of the loose ion pair, the lifetime of the contact ion pair increases with temperature. Using this model, the equilibrium constant K_5 (eq 6) can be determined from the experimental hfc constant, a, and the values of a_c and a_l obtained in the high- and low-temperature limits:[15]

$$K_5 = (a - a_l)/(a_c - a) \qquad (6)$$

The values of the hfc constants for the contact configuration can be taken from high-temperature data at 320−350 K (cf. Figure 4), i.e., $a_c(^7Li) = 1.06$ G and $a_c(^6Li) = 0.40$ G. The hfc's of the loose ion pair were determined by extrapolation to zero temperature, i.e., $a_l(^7Li) = 0.34$ G and $a_l(^6Li) = 0.20$ G. Within the temperature range of 167−250 K, the enthalpy, $\Delta H°$ = 1.5 kcal/mol, was calculated for both isotopes. The increase of $\Delta H°$ at temperatures above 250 K can be explained by the temperature dependence of the dielectric constant:[16,17]

$$K_5 \propto \exp(e^2/\epsilon r k T) \qquad (7)$$

where ϵ is the dielectric constant obeying $\epsilon = 1.49 - 2660/T$,[18] and r is the interion distance. This consideration results in a value of $r \approx 0.6$ Å, which is close to the Li^+ radius.[19] Although the above treatment of a Coulombic force model is true for point charges, we may conclude that practically, ion complexes are dominated by contact (tight) ion pairs, and thus, ET processes between ions, to be discussed below, may be rapid because of the geminate character of the interaction.

In view of the above discussion, the following equilibria are relevant throughout the following discussion:

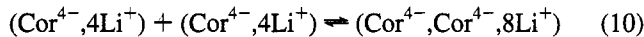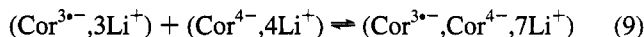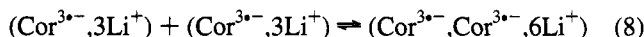(14) Atherton, N. M.; Weissman, S. I. *J. Am. Chem. Soc.* **1961**, *83*, 1330.
(15) Hirota, N. *J. Phys. Chem.* **1967**, *71*, 127.
(16) Szwarc, M., Ed. *Ions and Ion Pairs in Organic Reactions*; Wiley-Interscience: New York, 1972; Vol. 1, p 1.
(17) Fuoss, R. M. *J. Am. Chem. Soc.* **1958**, *80*, 5059.
(18) Hogen-Esch, T. E. *J. Am. Chem. Soc.* **1966**, *82*, 307.
(19) Weast, R. C. In *CRC Handbook of Chemistry and Physics*; CRC Press: Boca Raton, FL, 1990; Vol. 56, pp F-209.

$$(Cor^{3\bullet-},3Li^+) + (Cor^{3\bullet-},3Li^+) \rightleftharpoons (Cor^{3\bullet-},Cor^{3\bullet-},6Li^+) \qquad (8)$$

$$(Cor^{3\bullet-},3Li^+) + (Cor^{4-},4Li^+) \rightleftharpoons (Cor^{3\bullet-},Cor^{4-},7Li^+) \qquad (9)$$

$$(Cor^{4-},4Li^+) + (Cor^{4-},4Li^+) \rightleftharpoons (Cor^{4-},Cor^{4-},8Li^+) \qquad (10)$$

C. Electron Spin Polarization. a. Primary Excitation.

Whereas the dark electrochemical reactions may produce the monomer species with the diamagnetic dimer as an end product (eq 10), the dynamic processes following photoexcitation are initiated from the diamagnetic dimer $(Cor^{4-},Cor^{4-},8Li^+)$.

The main constituent of the Cor/Li/THF brown solution is the dimer $(Cor^{4-},Cor^{4-},8Li^+)$. Photoexcitation at 532 nm results in the spin-polarized EPR spectra attributed to the photoelectron, e^-_{photo}, and to $Cor^{3\bullet-}$ (Figure 5). The ESP effects were noticed within a temperature range of 176−230 K and Cor concentrations of $10^{-4}-10^{-3}$ M. No significant temperature-dependent changes in the spectra were detected at this temperature regime.

The intense single-line spectrum, which appears in emission immediately after the laser pulse, is attributed to e^-_{photo}, with $g_\epsilon = 2.0024 \pm 0.0002$ and the transverse relaxation time $T_{2e} = 0.7-1.0 (\pm 0.1) \mu s$. The signal decays to zero intensity with a characteristic time of $1.5 \pm 0.2 \mu s$. This value is of the same order of magnitude as the spin−lattice relaxation rate, T_{1e}, measured for the single-line spectrum of the photoelectron in pure Rb/THF solution.[20] The polarized multiplet in the spectra is attributed to $Cor^{3\bullet-}$ and exhibits exactly the same line positions as those obtained from the EPR spectrum of thermalized $Cor^{3\bullet-}$. This transient spectrum, in a net emissive mode, appears immediately after the laser pulse and strongly depends on the delay time between the laser and the microwave pulses, τ_d. Figure 6 depicts a rough estimate of the energy level diagram of free Cor^{4-} tetraanion, which is the main stable diamagnetic component of Cor/Li/THF brown solutions. This diagram, obtained from MNDO calculations,[21] is qualitative since it does not account for the dimer formation, as well as for the effects of the nearby lithium cations and the solvation shell of the multiparticle complex. Nevertheless, the energy gaps in the singlet manifold are in line with the experimental absorption spectrum of the brown Cor/Li/THF solution (cf. Figure 2).

Based on this qualitative energy scheme we assume that the primary photoexcitation occurs between S_0 and S_3 (or S_4) singlet states of Cor^{4-}:

$$(Cor^{4-},Cor^{4-},8Li^+) \xrightarrow{h\nu} (Cor^{4-},{}^{1*}Cor^{4-},8Li^+) \qquad (11)$$
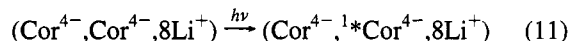
where ${}^{1*}Cor^{4-}$ stands for the excited singlet of the tetraanion. Near-resonant energy transfer (EnT) between pairs of tetraanions with formation of two nearby excited singlets, $(S_2 + S_2)$ or $(S_1 + S_2)$, is also feasible. These states may result in the triplet states $(T_2 + T_2)$, via intersystem crossing (ISC) followed by internal conversion to produce $(T_1 + T_1)$, i.e., $({}^{3*}Cor^{4-},{}^{3*}Cor^{4-},8Li^+)$. All these fast processes occur within the time period of the laser and microwave pulses and the assumed formation of two localized triplet tetraanions, complexed with eight lithium cations (cf. Figure 1), is essential to explain the spin polarized effects discussed below.[22]

b. Spin Polarization Mechanisms.

The brown solutions exhibit CIDEP effects as manifested by the net emissive spectra

(20) Rozenshtein, V.; Zilber, G.; Levanon, H. *J. Phys. Chem.* **1994**, *98*, 4236.
(21) Dewar, M. J. S.; Thiel, W. *J. Am. Chem. Soc.* **1977**, *99*, 4899.
(22) Other possibilities, such as $^3Cor^{4-}$ (or $^*Cor^{4-}$) paired to Cor^{4-} (ground or excited singlet), cannot be ruled out. However, these channels are irrelevant to the CIDEP effects discussed here.
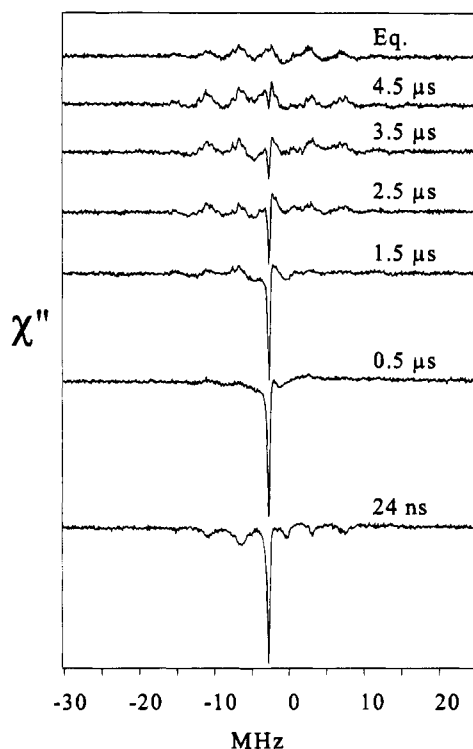
Figure 5. FT-EPR spectra of the photoexcited brown Cor/^{6}Li/THF solution vs the delay time, τ_d, between the laser and the microwave pulse ($T = 167$ K).
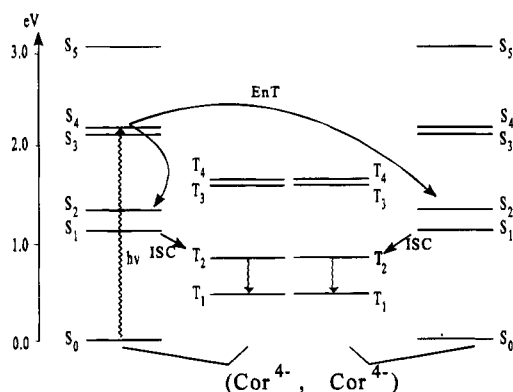
Figure 6. Energy level diagram of the separated constituents in the (Cor^{4-}, Cor^{4-}) (tetraanion pair) obtained by MNDO calculation. The initial excitation of a single Cor^{4-} within the pair is shared between the two constituents via energy transfer (EnT) as indicated by the arrows.

of the photoelectron and of the $Cor^{3\bullet-}$ radical trianion. We consider now several CIDEP mechanisms, that may contribute to the EPR spectra.

1. Triplet Mechanism. The triplet tetraanion $^3*Cor^{4-}$, which is formed in the primary processes, may react with one of the surrounding cations (within the dimer) to produce the polarized (pol) species via the triplet mechanism (TM):[23]

$$(^3*Cor^{4-}_{pol}, Li^+) \xrightarrow{ET} (Cor^{3\bullet-}_{pol}, Li^+, e^-_{photo,pol}) \quad (12)$$
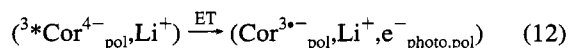
ISC selectively populates the triplet manifold of $^3*Cor^{4-}$ (in the molecular frame of reference), whose states are separated by the dipolar interaction in terms of the zero-field splitting (ZFS) parameters. If, indeed, the triplet polarization is formed, it can be conserved in the course of a fast reaction and, thus, can be transferred to the radical products. The ET rate (eq 12)

(23) Atkins, P. W.; Evans, G. T. *Mol. Phys.* **1974**, *27*, 1633.

must exceed 10^9 s^{-1} in order to compete with very rapid spin relaxation times of organic triplets ($T_{1T} \leq 10^{-9}$ s). For a geminate (Cor^{4-}, Li^+) ion pair, the rate of ET might be as large as 10^{13} s^{-1} (i.e., of the order of vibronic frequency) and does not depend upon reagent concentration. This is much larger than the spin relaxation rate. On the contrary, it can be too fast, causing line broadening of the triplet states and thus diminishing the selectivity of the ISC process. Although triplet polarization is inevitable in any triplet ← singlet ISC process, the restraints mentioned above make the TM less probable in our case.

2. S–T$_{-1}$ Radical Pair Mechanisms. Another possible CIDEP mechanism for the net emission of both radicals is the S–T$_{-1}$ RPM, which operates by mixing of the T$_{-1}$ state, containing only β electron spins, and the singlet state of the RP due to the magnetic interactions such as the hfc.[24] As a result, the electron and the nuclear spins flip simultaneously, producing net polarization, i.e., single-phase hyperfine-dependent polarization. In our case the RP is $(Cor^{3\bullet-}, e^-_{photo})$ and/or $(Cor^{3\bullet-}, Cor^{3\bullet-})$, formed via the reactions within the $(^3*Cor^{4-}, ^3*Cor^{4-}, 8Li^+)$ complex:

$$(^3*Cor^{4-}, ^3*Cor^{4-}, 8Li^+) \xrightarrow{ET}$$
$$(Cor^{3\bullet-}, e^-_{photo}, Cor^{3\bullet-}, e^-_{photo} 8Li^+) \quad (13)$$
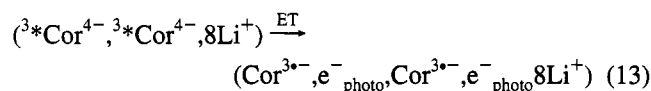
For an aggregate such as that on the righ-hand side of eq 13, which is tied together by Coulombic interaction of charged species, a very slow diffusion within the cage complex is expected. It implies a relatively long S–T$_{-1}$ mixing time. On the other hand, the hfc's of $Cor^{3\bullet-}$ are not so large (see above) for an effective energy level mixing. A strightforward recipe to check for an S–T$_{-1}$ RPM mechanism is by having the outermost hyperfine lines disappear. Unfortunately, the signal-to-noise ratio in the present experiments was insufficient to confirm an operative S–T$_{-1}$ RPM mechanism in the studied systems. On these grounds we cannot rule out this ESP mechanism, leaving this part of the analysis somewhat ambiguous.

3. Radical Triplet Pair Mechanism. To apply TM and S–T$_{-1}$ RPM, which were considered above, several conditions must be fulfilled. These restrictions can be avoided by considering ESP mechanisms that involve initially formed, unpolarized species (triplets and doublets), which exist within the time scale of our experiments. In the presently discussed systems, the triplet–triplet and radical–triplet pairs are generated within the cage, and their mutual interaction seems to be inevitable.

A recently proposed polarization mechanism known as radical–triplet pair mechanism, RTPM,[25–28] may be the most pertinent mechanism for explaining the results of the ESP effects in the brown solutions, where the dimer $(^3*Cor^{4-}, ^3*Cor^{4-}, 8Li^+)$ is suggested to exist. As we shall see below, unlike TM and S–T$_{-1}$ RPM, the requirement for an initial polarized triplet precursor is not essential, thus simplifying the analysis of the ESP effects. For a coherent presentation we first start with a qualitative description of the RTPM (Figure 7). The overall scheme of doublet–triplet interaction for a geminate pair can be depicted by the reaction sequence presented schematically:
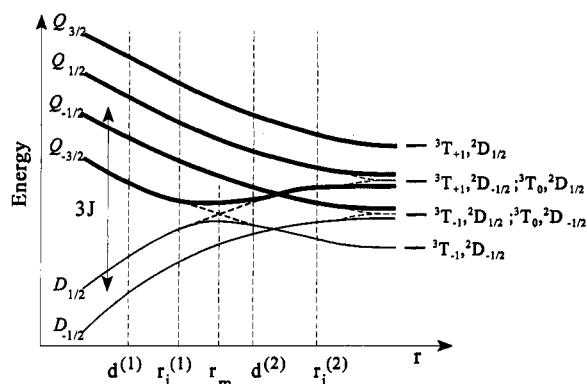
(24) Salikhov, K. M.; Molin, Y. N.; Segdeev, R. Z.; Buchachenko, A. L. *Spin Polarization and Magnetic Effects in Radical Reactions*; Elsevier: Amsterdam, 1984.
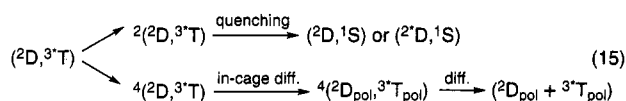(25) Blättler, C.; Jent, F.; Paul, H. *Chem. Phys. Lett.* **1990**, *166*, 375.
(26) Kawai, A.; Okutsu, T.; Obi, K. *J. Phys. Chem.* **1991**, *95*, 9130.
(27) Kawai, A.; Obi, K. *Res. Chem. Intermed.* **1993**, *19*, 865.
(28) Shushin, A. I. *Chem. Phys. Lett.* **1993**, *208*, 173.

Figure 7. Energy correlation diagram of the doublet−triplet pair. The terms on the left-hand side denote pair states, and those on the right-hand side are ascribed to the separated species.

$$(^{3*}T,^{3*}T) \xrightarrow{ET} (^2D,^{3*}T) \quad (14)$$

$$(^2D,^{3*}T) \begin{cases} 2(^2D,^{3*}T) \xrightarrow{\text{quenching}} (^2D,^1S) \text{ or } (^{2*}D,^1S) \\ 4(^2D,^{3*}T) \xrightarrow{\text{in-cage diff.}} {}^4(^2D_{pol},^{3*}T_{pol}) \xrightarrow{\text{diff.}} (^2D_{pol} + {}^{3*}T_{pol}) \end{cases} \quad (15)$$

where $^2D = Cor^{3*-}$ or e^-_{photo}, $^{3*}T = {}^{3*}Cor^{4-}$, and the mixing $^2(^2D,^{3*}T) \leftrightarrow {}^4(^2D,^{3*}T)$ occurs via magnetic interactions (Zeeman, ZFS, and hfc.).

An ET reaction between $^{3*}T$ and Li^+ results in the geminate doublet−triplet pair $(^2D,^{3*}T)$. In terms of the energy level diagram (Figure 7), the doublet−triplet initial separation distance, r_i, can be either $r_i^{(1)} < r_m$ or $r_i^{(2)} > r_m$, where r_m is the distance at the energy states mixing. At short separation distances, the coupled doublet−triplet spin states of the pair splits through the exchange interaction, J, into a quartet, $S = {}^3/_2$, and a doublet, $S = 1/2$, i.e., into $Q \equiv {}^4(^2D,^{3*}T)$ and $D \equiv {}^2(^2D,^{3*}T)$, respectively. In the course of the motion within the complex, the distance between the constituents $(^2D,^{3*}T)$, within the pair, can fluctuate, thus affecting the values of J. It is important to note that Q and D states behave differently. In terms of eq 15, the quartet pair, over the entire in-cage separation range, maintains the same constituents and also conserves its quartet characters while the doublet pair does not fulfill these conditions. In the case of the doublet pair $^2(^2D,^{3*}T)$, the triplet constituents, $^{3*}T$, undergo the irreversible quenching process to produce new doublet pairs $(^2D,^1S)$ or $(^{2*}D,^1S)$.

Two mechanisms of triplet quenching are allowed. The first is the singlet ← triplet ISC, enhanced by the interaction with the doublet,[29] and the second is the electronic energy transfer from the triplet to the doublet molecule.[30] The former mechanism occurs via ISC induced by the electron exchange or the charge-transfer interaction and leads to dissipation of the electronic energy of the triplet over the vibronic manifold of the final pair $(^2D,^1S)$. The rate of ISC strongly depends upon the energy gap between the initial triplet and the ground singlet state, $\Delta E = E_T - E_S$:[29,31]

$$k_{ISC} = 2|H_{ex}|^2 F/\hbar H_v \quad (16)$$

where H_{ex} is the matrix element of the exchange interaction, F is the Frank−Condon factor, and H_v^{-1} is the density of the final states. For aromatic hydrocarbons, $F = 0.15 \times \exp\{-(\Delta E - 4000)/2175\}$[32] ($\Delta E$ in cm^{-1}). Since these vibronic states are

coupled to the energy states of the solvent, the vibrational energy transfer to the bulk should occur very effectively, without affecting the overall relaxation rate, i.e., within $\sim 10^{-12}$ s,[31] which corresponds to $H_v \sim 10 \ cm^{-1}$. Having $\Delta E \cong 4000 \ cm^{-1}$ (cf. Figure 6), $H_{ex} \cong 50 \ cm^{-1}$,[31] and $H_v \cong 10 \ cm^{-1}$, k_{ISC} was calculated to be $\cong 10^9$ s^{-1}. For an ion-bound pair, as that discussed here, diffusion within the cage should be restricted to at least $D_{dif} \sim 10^{-7} \ cm^2$/s, with $r_i \sim 5 \ Å$.[33] Therefore, the collision complex $(^2D,^{3*}T)$ may exist during the time period, τ_c, of $\sim r_i^2/D_{dif} \sim 10^{-8}$ s. Comparing k_{ISC}^{-1} with τ_c indicates that the diffusion is sufficiently slow, thus allowing for the enhanced ISC mechanism.

The second possible quenching mechanism is the energy transfer model, where the triplet transfers its electronic energy to excite the doublet.[30] MNDO calculations, carried out for the Cor^{3*-} radical, indicate that the lowest-lying excited doublet state (0.45 eV) is in resonance with the photoexcited triplet, $^{3*}Cor^{4-}$.

Polarization: In terms of eq 15 and Figure 7 the triplet quenching mechanisms are rapid enough to depopulate $D_{1/2}$ and $D_{-1/2}$ radical−triplet pair states immediately after their generation, i.e., within the time constant of the experimental setup. Consequently, we can consider the populated quartet states, Q, to be the precursors for the spin polarization as will be discussed below. For simplicity, let us assume that all quartet states are equally populated. Upon its creation, the quartet pair, $^4(^2D,^{3*}T)$, separates along the potential surfaces represented schematically in Figure 7. These quartet pairs may acquire a doublet character by the magnetic interactions, such as (1) the hfc of ^2D, (2) the difference between Zeeman interactions of ^2D and $^{3*}T$, and (3) the dipolar (ZFS) interaction of $^{3*}T$. We discuss only the ZFS interaction, which is dominant. For organic triplets in frozen matrices, its value is about 1000 G, which corresponds to a $Q-D$ state-mixing time of about 3×10^{-10} s. In liquids, this value may be longer because of motional averaging, thus reducing the mixing time to some extent. However, a cage lifetime of 10^{-8} s, as calculated here, is much longer than the state-mixing time, ensuring an effective mixing process in the alkali-metal complexes.

The states Q_i ($i = 1/2, 3/2$) and D_j ($j = 1/2$) are mixed by the dipolar interaction at two interspin distances that are of interest. First, at the avoided crossing ($r = r_m$), the states $Q_{-3/2}$ and $D_{1/2}$ are mixed, and second, at $r = r(J \rightarrow 0)$, the states, $Q_{1/2}$ and $D_{1/2}$ as well as $Q_{-1/2}$ and $D_{-1/2}$ are mixed.[25-28] Energy state mixing at $r(J \rightarrow 0)$ cannot induce spin polarization, since mixed radical−triplet pair states correlate with states of the separated species, possessing equal amounts of α and β spins. Thus, with the triplet quenching mechanism, only the avoided crossing at $r = r_m$ results in a polarization effect through the adiabatic passage (Figure 7). Depending on the mutual values of r_m, r_i, and the distance of closest approach, d, two different cases of RTPM associated with state mixing and relaxation processes are considered.[25-28]

Case 1: The initial separation distance is smaller than the energy intersection distance, i.e., $r_i = r_i^{(1)} \leq r_m$.[25-27] Because of the quartet−doublet mixing, the initially generated quartet pairs evolve adiabatically along the potential curves. At large separation distances the quartet states correlate with the triplet and doublet states of the separated species, i.e., $Q_{3/2}$ with $(^3T_{+1} + {}^2D_{1/2})$, $Q_{1/2}$ and $Q_{-3/2}$ with $(^3T_{+1} + {}^2D_{-1/2} + {}^3T_0 + {}^2D_{1/2})$, and $Q_{-1/2}$ with $(^3T_{-1} + {}^2D_{1/2} + {}^3T_0 + {}^2D_{-1/2})$. Consequently, the above states are being populated, while the $(^3T_{-1} + {}^2D_{-1/2})$

(29) Gijzeman, O. L. J.; Kaufman, F.; Porter, G. *J. Chem. Soc., Faraday Trans. 2* **1973**, *95*, 9130.
(30) Kuzmin, V. A.; Tatikolov, A. S. *Chem. Phys. Lett.* **1978**, *53*, 606.
(31) Hoijtink, G. J. *Acc. Chem. Res.* **1969**, *2*, 114.
(32) Siebrand, W. *J. Chem. Phys.* **1967**, *47*, 2411.

(33) This estimation is based upon normal conditions, in which $D_{dif} \sim 10^{-5} - 10^{-6} \ cm^2$/s for free diffusion in liquid. In our case, $D_{diff} < 10^{-6} \ cm^2$/s.

state remains unpopulated, since it correlates with the empty $D_{1/2}$ pair state. The overall deficiency of the β spins should results in a net emissive polarization.

Case 2: Here, the RTPM is developed at distances beyond the avoided crossing. In this case the distance of closest approach exceeds the distance of energy state mixing, i.e., $r_i = r_i^{(2)} \geq d^{(2)} \geq r_m$ (Figure 7). For such a case, where the exchange interaction is comparable with the Zeeman energy, the relaxation model of RTPM was proposed.[28] In this model, the rotational motion of the triplet modulates the dipolar (ZFS) interaction to induce spin–lattice relaxation. Therefore, the net ESP is produced by the transitions whose probabilities are different and related to the modified energy gaps affected by the exchange interaction between the quartet and doublet states. Thus, the rates of $Q_{3/2} \rightarrow D_{1/2}$, $Q_{3/2} \rightarrow D_{-1/2}$, and $Q_{1/2} \rightarrow D_{-1/2}$ transitions are reduced (larger gaps) and the rates of $Q_{-3/2} \rightarrow D_{-1/2}$, $Q_{-3/2} \rightarrow D_{1/2}$, and $Q_{-1/2} \rightarrow D_{1/2}$ transitions are increased (smaller gaps) (cf. Figure 7). For the case where $J < \omega_L$, the net spin polarization (P_{RTPM}) caused by the different relaxation rates within the $Q \rightarrow D$ transitions discussed above is expressed by:[28]

$$P_{RTPM}(J<\omega_L) \propto -D_{ZFS}^2 D_{rot}/D_r \qquad (17)$$

where D_{rot} is the diffusion coefficient for the rotation of ^3T and D_r is the diffusion coefficient of the relative motion of the triplet doublet pair within the complex. Since $D_{rot} \propto T/\eta$ and $D_r \propto T/\eta$,[34] the polarization does not depend upon temperature and viscosity, as confirmed by our observations.[35]

At this stage, we are unable to state whether the mixing and/ or the relaxation processes account for the polarization. Nevertheless, if the polarization is governed by the relaxation mechanism, $J < \omega_L$ should be considered appropriate in our photoexcited Cor/Li/THF system. The same conclusion was derived earlier by Goudsmit et al.[36] where RTPM was observed in photoexcited TEMPO/benzophenone solutions.

IV. Concluding Remarks

The initially generated triplet–triplet pairs and radical products (Cor$^{3\bullet-}$ and e$^-_{photo}$) participate in the spin dynamics, inducing the net emissive polarization. This is probably the first case where the spin polarization was detected in ion complexes with highly charged components. The specific magnetic effects are driven, to some extent, by the electrical forces within the ionic cluster (up to ten charged species). The CIDEP effects associated with these systems are discussed within the framework of traditional and relatively novel polarization mechanisms. We believe that the RTPM, which is of general interest in CIDEP phenomena, explains smoothly the experimental results. Moreover, the spin dynamics and photochemistry of ion-bound complexes as revealed by the alkali-metal–polyanion systems is of particular interest, as they may be considered as bridging systems between freely diffusing and fixed distance donor–acceptor systems.

(34) Jones, L. L.; Schwarz, R. N. *Mol. Phys.* **1981**, *43*, 52.

(35) For $J > \omega_L$, a strong temperature dependence is expected and the polarization is expressed by: $P_{RTPM}(J > \omega_L) \sim -D_{ZFS}^2/D_r k \sim -D_{ZFS}^2/kT$, where $k = 1-3$ (see ref 28).

(36) Goudsmit, G.-H.; Paul, H.; Shushin, A. I. *J. Phys. Chem.* **1993**, *97*, 13243.